

Confining the Angular Distribution of TGF Emission

Thomas Gjesteland¹, Nikolai Østgaard¹, Andrew B. Collier^{2,3}, B. E. Carlson¹, M. B. Cohen⁴, N. G. Lehtinen⁴

¹Physics and Technology, University of Bergen, Postboks 7803, Bergen, 5020, Norway
thomas.gjesteland@uib.no

²Hermanus Magnetic Observatory, Hermanus, South Africa

³School of Physics, University of KwaZulu-Natal, Westville Campus, Durban,, South Africa

⁴STAR Laboratory, Stanford University, Stanford, CA, USA

Abstract

We present the first constraints on the TGF emission cone, based on accurately geolocated TGFs. The distribution of the observation angles for 106 TGFs are compared to Monte Carlo simulations. We find that TGF emissions within an isotropic half angle $>30^\circ$ can generate the observations. In addition, 36 events are used for spectral analysis. The result is a significant softening of the TGF energy spectrum for large observation angles, which is consistent with a TGF emission half angle $<40^\circ$. The constraints $30^\circ - 40^\circ$ indicates that the electrons which produce TGFs are accelerated in nearly vertical electric fields.

1. Introduction

Terrestrial gamma ray flashes (TGFs) are short (~ 1 ms) gamma emission from the Earth's atmosphere, which were proposed nearly a century ago [1] and later discovered by the Burst and Transient Source experiment (BATSE) on board the Compton Gamma Ray Observatory (CGRO) [2]. TGFs are assumed to be bremsstrahlung emission from relativistic electrons which are accelerated in electric fields related to thunderstorms. Several studies have determined the production altitude of TGFs, detected by satellite instruments, to be ~ 15 - 20 km altitude [e.g 3-6], which indicates that TGFs originate in the upper troposphere, probably inside thunderclouds.

The geometry of the initial gamma emission is sketched in Figure 1. In the following we will call the half angle of the gamma emission θ , and the angle between the satellite nadir and the straight line to the TGF source α . The nature of the initial gamma emission is still under debate. Studies have suggested a wide ($\theta \sim 45^\circ$) emission cone [3,5], and a wide non-isotropic emission [7].

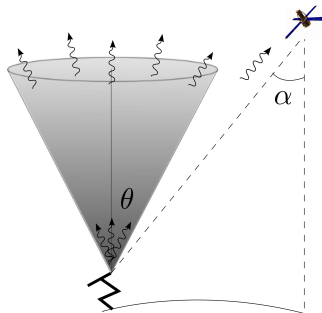


Figure 1: A sketch of the TGF emission cone with half angle θ and the satellites observation angle α .

2. Gamma production and propagation in the atmosphere

Electrons are accelerated by electric and magnetic fields. As long as the electron collision frequency is significantly larger than the gyro frequency the motion of the electron are predominantly in the direction of the

electric field. The effect of the magnetic field on the electron is negligible at altitudes below 20 km [8]. As a result the electrons motion are align the electric field. Relativistic electrons emits bremsstrahlung predominantly in the forward direction. This is shown by the Bethe-Heitler formula. From a MC simulation it is shown that the gamma emission from relativistic breakdown in a parallel electric field is beamed and drops one order of magnitude at $\sim 30^\circ$ off axis [7].

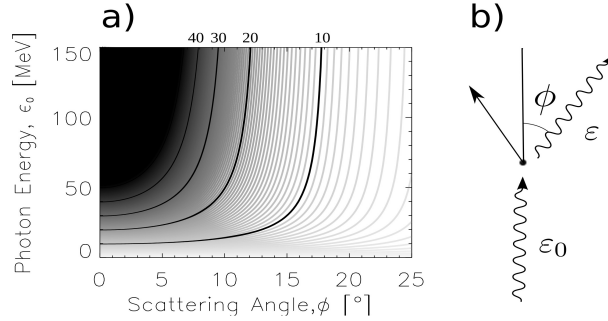


Figure 2: a) Energy reduction as a function of scattering angle. Y-axis is the energy before scattering and the contour curves represent photon energy after Compton scattering: 10 MeV, 20 MeV, 30 MeV, and 40 MeV contours are labelled. b) Compton scattering schematics.

Gamma-photon flux propagating in air is attenuated, the most important interactions for photon energies in the range 10 keV-40MeV being the photoelectric absorption, Compton scattering and pair production. Photoelectric absorption is almost negligible for photon energies above 100 keV and pair production is only effective for energies above 1.22 MeV. While in the photoelectric effect, the photons are absorbed with a production of an electron, in the pair production process, both an electron and a positron are created. Compton scattering is effective for all photon energies and results in scattering of the photon momentum and a degeneration in the photon energy. The reduction in photon energy is dramatic for large scattering angles. Figure 2 shows the scattering angle as a function of initial photon energy when the photon energy after scattering is given. If the photon energy after scattering is 10 MeV it cannot have been scattered by more than 18° , assuming the photon energy before interaction is <150 MeV. If the final energies are higher, i.e. 20 MeV, 30 MeV or 40 MeV, the scattering angle is $<\sim 10^\circ$. If a TGF is detected outside the emission cone only scattered photons will be seen, and the TGF energy spectrum should have a fall off at higher energies.

3. Angular distribution of TGFs

This study have used 106 TGFs detected by the Reuven Ramaty High Energy Solar Spectroscopic Imager (RHESSI) which have been geolocated by the AWESOME network [9] and the World Wilde Lightning Location Network (WWLLN) [10]. The observation angle distribution of these measurements is compared to calculated distributions from Monte Carlo (MC) simulations of TGF through the atmosphere. The MC simulation is described in [11]. In the simulations the production altitude and initial emission angle are chosen. We also assumes that the number of initial photons in a TGF is distributed according to a power law with spectral index, k . In each run we assume the TGF to occur randomly below the satellites. Figure 3 shows the observation angle distribution from the RHESSI measurements as a histogram. The best fit distribution from our simulations with various half angles is also shown. Half angle of $\theta=30^\circ$ with $k=2.0$ is solid, $\theta=40^\circ$ with $k=2.1$ is dotted and $\theta=60^\circ$ with $k=2.3$ is dashed. Figure 3 shows that $\theta>30^\circ$ can best represent the observed distribution.

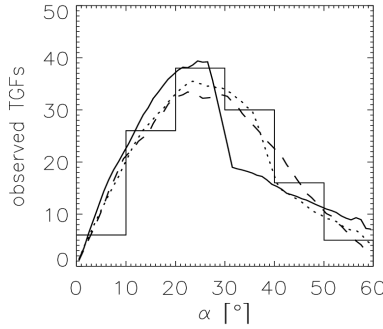


Figure 3: The histograms show the distribution of geolocated TGFs per observation angle, α . The curves are the best results from MC simulations with $\theta=30^\circ$, $k=2.0$ (Solid), $\theta=40^\circ$, $k=2.1$ (dotted) and $\theta=60^\circ$, $k=2.3$ (dashed). The calculations were performed for the TGF source altitude of 15 km.

4. Spectral analysis of TGF observed at large angles

The energy spectrum of the TGFs can give us further information on the TGF emission cone. From the total set of the TGFs with corresponding geolocated sferics, 36 occurred before the radiation damage to the RHESSI instrument in early 2006 [12], and only events occurring before this are valid for proper spectral analysis. We have used the data and detector response matrix (DRM) from the RHESSI TGF catalog [12]. For each RHESSI TGF, the detected photons are too few to perform spectral analysis. Therefore we have divided the measurements from these 36 TGFs into three spectra each with a 20° observation angle bin. Figure 4a shows each energy spectrum with the average number of counts and the error bars representing one standard deviation of the mean value. Figure 4a shows that RHESSI measures a significant softening of the energy spectrum in the 40° - 60° bin versus the two others since the first energy bin has significantly more counts and the two highest energy bins have significantly fewer counts. There is also a trend that the 20° - 40° spectrum is softer than the 0° - 20° spectrum since it has significantly fewer counts in the highest energy bin.

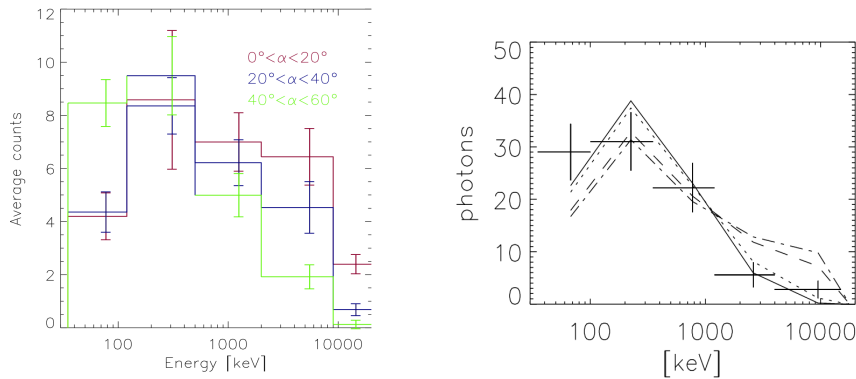


Figure 4: a) The average energy spectrum for various observation angles, α . The $40^\circ < \alpha < 60^\circ$ spectrum has significantly more counts in the lowest energy bin and significantly fewer counts in the two highest energy bins compared to the others. b): Combined energy spectrum from 10 RHESSI TGFs and the energy spectrum from MC-simulations with $\theta=30^\circ$ (solid), $\theta=40^\circ$ (dotted), $\theta=50^\circ$ (dashed) and $\theta=60^\circ$ (dot dashed). production altitude of 15 km. The simulated spectra are normalized to the RHESSI measurements

Figure 4b shows a combined energy spectrum of the 10 RHESSI TGFs observed at $\alpha > 40^\circ$, which corresponds to more than ~ 500 km between the TGF production and the sub-satellite point. The simulated spectra in Figure 4b are results from our MC simulations folded through the RHESSI DRM. Simulated TGFs with $\theta=50^\circ$ or $\theta=60^\circ$ do not have a high energy fall off which is found in the RHESSI measurements. A narrower emission cone fits the measurements, which indicates that $\theta < 40^\circ$.

4. Summary

We have used accurate geolocation of RHESSI TGFs to confine the angular TGF emission. When assuming an isotropic emission cone the half angle is confined to $30^\circ < \theta < 40^\circ$, which is in agreement with earlier studies [3,5,7]. $30^\circ < \theta < 40^\circ$ indicate that TGFs are produced in a vertical or slightly divergent (up to 20° from vertical) electric field. Our simulations shows that it is likely to detect TGFs at $\alpha > 50^\circ$ which corresponds to $>700\text{km}$ between the source spheric and the sub-satellite point. We have also found that TGFs detected at $\alpha > 40^\circ$ have a significantly softer energy spectrum, which is the result of Compton scattering.

5. References

- [1] C. T. R. Wilson, "The electric field of a thundercloud and some of its effects", Proc.Phys. Soc. London, 1925.
- [2] G. J. Fishman, P.N. Bhat, R. Mallozzi, J.M. Horack, T. Koshut, C. Kouveliotou, G.N. Pendleton, C.A. Meegan, R.B. Wilson, W.S. Paciasas, S.J. Goodman, and H.J. Christian, "Discovery of Intense Gamma-Ray Flashes of Atmospheric Origin," *Science*, vol. 264, May. 1994, pp. 1313-1316.
- [3] J.R. Dwyer, and D. M. Smith, "A comparison between monte carlo simulations of runaway breakdown and terrestrial gamma-ray flash observations", *Journal of Geophysical Research*, doi:10.1029/2005GL023848, 2005.
- [4] E. Williams, , et al., "Lightning flashes conducive to the production and escape of gamma radiation to space", *Journal of Geophysical Research (Atmospheres)*, 111 (D10), D1609, doi:10.1029/2005JD006447, 2006.
- [5] B.E. Carlson, N. G. Lethinen, and U. S. Inan, "Constraints on terrestrial gamma ray flash production from satellite observation", *Geophys. Res. Lett*, 34, L08809, doi:10.1029/2006GL029229, 2007.
- [6] T. Gjesteland, N. Østgaard, P. H. Connell, and G. J. Fishman, "Effects of dead time losses on terrestrial gamma ray flash measurements with the burst and transient source experiment", *J. Geophys. Res.*, 115, doi:10.1029/2009JA014578, 2010.
- [7] B. J. Hazelton, B. W. Grefenstette, D. M. Smith, J. R. Dwyer, X.-M. Shao, S. A. Cummer, T. Chronis, E. H. Lay, and R. H. Holzworth, "Spectral dependence of terrestrial gamma-ray flashes on source distance", *Geophys. Res. Lett.*, 36, L01108, doi:10.1029/2008GL035906, 2009.
- [8] A.V. Gurevich, A. V., J. A. Valdivia, G. M. Milikh, and K. Papadopoulos, "Runaway electrons in the atmosphere in the presence of a magnetic field", *Radio Sci.*, 31(6), 1541–1554, doi:10.1029/96RS02441, 1996.
- [9] M.B. Cohen, U.S. Inan, R.K. Said, and T. Gjesteland, "Geolocation of terrestrial gamma-ray flash source lightning," *Geophysical Research Letters*, vol. 37, 2010, p. L02801.
- [10] A. B. Collier, T. Gjesteland and N. Østgaard, "Assessing the Power Law Distribution of TGFs", to be submitted, 2011.
- [11] N. Østgaard, T. Gjesteland, J. Stadsnes, P. Connell, and B. Carlson, "Production altitude and time delays of the terrestrial gamma flashes: Revisiting the burst and transient source experiment spectra", *J. Geophys. Res.*, doi:10.1029/2007JA012618, 2008.
- [12] B.W. Grefenstette, D.M. Smith, B.J. Hazelton, and L.I. Lopez, "First RHESSI terrestrial gamma ray flash catalog," *Journal of Geophysical Research*, vol. 114, 2009.